# Superconductivity in type-II Weyl semimetals

M. Alidoust, K. Halterman, and A. A. Zyuzin

Phys. Rev. B **95**, 155124 — Published 17 April 2017

DOI: 10.1103/PhysRevB.95.155124

# Superconductivity in Type-II Weyl Metals

M. Alidoust,[1] K. Halterman,[2] and A. A. Zyuzin[3,4]

[1] *Department of Physics, Faculty of Sciences, University of Isfahan, Hezar Jerib Avenue, Isfahan 81746-73441, Iran*
[2] *Michelson Lab, Physics Division, Naval Air Warfare Center, China Lake, California 93555*
[3] *Department of Physics, KTH-Royal Institute of Technology, Stockholm, SE-10691 Sweden*
[4] *Ioffe Physical–Technical Institute, 194021 St. Petersburg, Russia*

We study superconductivity in a Weyl semimetal with a tilted dispersion around two Weyl points of opposite chirality. In the absence of any tilt, the state with zero momentum pairing between two Fermi sheets enclosing each Weyl point has four point nodes in the superconducting gap function. Moreover, the surface of the superconductor hosts Fermi arc states and Majorana flat bands. We show that a quantum phase transition occurs at a critical value of the tilt, at which two gap nodes disappear by merging at the center of the first Brillouin zone, or by escaping at its edges, depending on the direction of the tilt. The region in the momentum space that the Majorana flat band occupies is found to increase as the tilt parameter is made larger. Additionally, the superconducting critical temperature and electronic specific heat can be enhanced in the vicinity of the quantum phase transition due to the singularity in the electronic density of states.

PACS numbers: 74.25.Dw, 03.65.Vf, 71.90.+q

## I. INTRODUCTION

Weyl semimetals and the closely related Dirac semimetals are topologically nontrivial phases of matter which were first predicted theoretically [1–5] and recently realized experimentally in TaP, NbP, TaAs, NbAs, $Cd_3As_2$, $Na_3Bi$, and $ZrTe_5$ [6–16]. The band structure of these materials contains nondegenerate conduction and valence bands touching at certain "Weyl points", around which, the energy dispersion of the quasiparticle excitations is linear. The corresponding three dimensional conical band structure in this part of the spectrum is referred to as a Weyl cone. The Weyl points which always come in pairs, represent a source or a sink of Berry curvature in the momentum space, and describe Weyl fermions in real space [17]. Although the band structure in the bulk of Weyl semimetals is gapless, the bulk-edge correspondence gives rise to Fermi arc surface states that connect pairs of Weyl points.

It was found that the tilt of the Weyl cone results in a Lifshitz transition, whereby the point-like Fermi surface transforms into a series of electron and hole Fermi pockets connected to each other by a single point [18]. This is the so-called type-II phase of a Weyl semimetal [19]. The tilt of the Weyl cone can be realized, for example, by applying strain to the crystalline Weyl semimetal structure [20] or a Zeeman field [21]. The electronic transport in Weyl semimetals with tilted Weyl cones including conductance [22], chiral anomaly [19], and intrinsic anomalous Hall effect [23] become anisotropic compared to an ideal Weyl semimetal.

Superconductivity in Weyl metals may give rise to topological phases that host Majorana fermions. This has triggered a great deal of interest both experimentally and theoretically due to the possible applications in quantum computation [24]. In general, one expects zero-momentum inter-valley pairing and finite momentum intra-valley pairing in Weyl metals due to the multiple number of valleys within its band structure [25–29]. It was argued that inter-valley pairing can be energetically more favorable than intra-valley pairing, provided time reversal symmetry is violated, but inversion symmetry is preserved [28]. If such a condition is realized, the superconducting gap exhibits four nodes with Majorana surface states that connect projections of the node locations onto the surface of the Brillouin zone, as well as Fermi arc surface states that connect two distinct Fermi sheets [25, 27–29].

In this paper, our objective is to theoretically investigate superconductivity in type-II Weyl metals. Motivated primarily by the recent experimental observations of a type-II Weyl semimetal state [30–35], and pressure enhanced superconductivity [36] in the type-II Weyl semimetal candidate $MoTe_2$, we investigate the zero momentum inter-valley superconducting state in a Weyl semimetal with tilted conical spectrum around the Weyl points. We show that if the cone tilts in same direction as along the two Weyl points, then there can be a critical tilt orientation in which a quantum phase transition occurs. At this phase transition, the two nodes in the superconducting gap function disappear by merging at the center of the first Brillouin zone or by escaping at the Brillouin zone edges, depending on whether the Weyl cones are tilted towards or away from each other. Interestingly, while the Fermi arc surface states tend to defined hybridize with the bulk bands in the Weyl superconductor, the region of momentum space where the Majorana band is flat becomes expanded by increasing the tilt angle. The phase transition can also have a number of profound effects, including an enhancement of the superconducting critical temperature and electronic specific heat arising from the Van-Hove singularity in the

electronic density of states.

The rest of the paper is organized as follows: In Sec. II, we first introduce the low-energy model used for a Weyl superconductor with tilted conical spectrum, and calculate the temperature at which the superconductor-metal phase transition occurs for various limits of the tilt. In Sec. III we analyze the spectrum of both the bulk and surface states in this system analytically. In Sec. IV, we extend our analysis of the surface states by implementing exact numerical and diagonalization techniques. Finally, in Sec. V, we present a summary of our results and give concluding remarks.

## II. MODEL AND THERMODYNAMIC PROPERTIES

We consider a minimal model for a Weyl semimetal with only two valleys in the band structure and a Weyl point in each valley [4]. This model can be described by $H = \int \frac{d^3k}{(2\pi)^3} c^\dagger_{\mathbf{k}} H(\mathbf{k}) c_{\mathbf{k}}$, where the momentum space Hamiltonian is given by,

$$H(\mathbf{k}) = v_z(\sigma_z + \alpha\tau_z + \beta)(k_z\tau_z - Q) + v_\perp[\hat{\boldsymbol{z}} \times \boldsymbol{\sigma}] \cdot \mathbf{k}, \quad (1)$$

where $\boldsymbol{\sigma}$ and $\boldsymbol{\tau}$ are vectors composed of the three Pauli matrices acting on the spin and valley degrees of freedom respectively, and $2Q$ is the separation of the two Weyl cones along the $z$-axis in the momentum space. The parameters $\alpha$ and $\beta$ describe the tilt of the two Weyl cones that are either in the same direction or the opposite direction with respect to each other, and $v_z, v_\perp$ are the components of the anisotropic Fermi velocity when the tilt parameters vanish. We represent the annihilation operator $c_{\mathbf{k}}$ as $c_{\mathbf{k}} \equiv [c_{\mathbf{k},\uparrow,R}, c_{\mathbf{k},\downarrow,R}, c_{\mathbf{k},\uparrow,L}, c_{\mathbf{k},\downarrow,L}]^{\mathrm{T}}$, for electrons with momentum $\mathbf{k}$ and spin $\uparrow,\downarrow$, in the two valleys denoted by $R, L$.

We consider the case where the direction of tilt is along the direction in which the two Weyl points are separated, resulting in nontrivial behavior of the nodes in the gap function of the Weyl superconductor. We also consider the limit $\alpha = 0$, focusing on the effects of tilting the Weyl cones in opposite directions with respect to each other. The effects of finite values of $\alpha$ are discussed in Sec. V.

Let us recall the band structure of a Weyl semimetal as a function of the tilt parameter. For slight tilting with $|\beta| < 1$, the band-structure of the system consists of two valleys where the electron and hole bands touch each other at a Weyl point in both valleys. These two point nodes are separated by $2Q$ along the $z$-axis in the momentum space. With increasing tilt, one can reach a situation where $|\beta| = 1$, at which the two Weyl points transform into a nodal line that coincides with the $z$-axis. By increasing the tilt further such that $|\beta| > 1$, the nodal line transform into electron and hole Fermi pockets connected to each other by the point nodes.

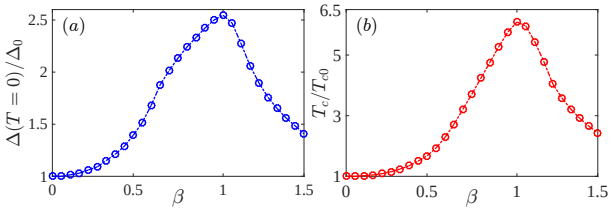


FIG. 1. (Color online) Tilt parameter $\beta$ dependence of: (a) order parameter $|\Delta|/|\Delta_0|$ at zero temperature and (b) critical temperature $T_c/T_{c0}$, which are normalized to their values in the case $\beta = 0$.

We now consider inversion symmetric inter-valley s-wave superconducting pairing, which can be described by $H = \frac{1}{2}\int \frac{d^3k}{(2\pi)^3} \psi^\dagger_{\mathbf{k}} \mathcal{H}(\mathbf{k}) \psi_{\mathbf{k}}$, where $\psi_{\mathbf{k}} = [c_{\mathbf{k}}, c^\dagger_{-\mathbf{k}}]^{\mathrm{T}}$ is the Nambu spinor and the BCS Hamiltonian is given by

$$\mathcal{H}(\mathbf{k}) = \begin{pmatrix} H(\mathbf{k}) - \mu & i\sigma_y\tau_x\Delta \\ -i\sigma_y\tau_x\Delta^* & -H^{\mathrm{T}}(-\mathbf{k}) + \mu \end{pmatrix}, \quad (2)$$

where $\mu$ is the Fermi energy and $\Delta$ is the spatially homogeneous inter-valley $s$-wave order parameter, which is defined by a solution of the self-consistency equation,

$$\Delta = \frac{\lambda T}{4} \sum_{n\in\mathbb{Z}} \sum_{s=\pm 1} \int \frac{d\mathbf{k}}{(2\pi)^3} \frac{\Delta}{\omega_n^2 + E_s^2(\mathbf{k})} \times \left[1 + s\frac{v_z^2 k_z^2}{\sqrt{|\Delta|^2 v_z^2 k_z^2 + (\mu - \beta v_z k_z)^2 \epsilon^2(\mathbf{k})}}\right]. \quad (3)$$

Here $\lambda > 0$ is the interaction constant, which is assumed to be independent from the tilt parameters, $T$ is the temperature, and $\omega_n = \pi T(2n+1)$ is the Matsubara frequency. We also have $\epsilon(\mathbf{k}) = \sqrt{v_z^2 k_z^2 + v_\perp^2(k_x^2 + k_y^2)}$, and dispersion of quasiparticles

$$E_s^2(\mathbf{k}) = \epsilon^2(\mathbf{k}) + |\Delta|^2 + (\mu - \beta v_z k_z)^2 + 2s\sqrt{\epsilon^2(\mathbf{k})(\mu - \beta v_z k_z)^2 + v_z^2 k_z^2 |\Delta|^2}, \quad (4)$$

which clearly has nodes along $z$-axis in momentum space at $\beta = 0$.

We emphasize that we are interested in the most simplest case of s-wave phonon mediated superconductivity in Weyl metals discussed in Ref. [28]. Particularly, it was shown that the intra-valley pairing is less energetically favorable than the inter-valley one provided that the inversion symmetry is preserved. We now extend that theory to Weyl metals with tilted cones. The inversion symmetry is preserved if two Weyl cones are not tilted in the same directions with respect to each other, which allows us to conclude that the inter-valley pairing is the dominant pairing in the presence of tilt parameter $\beta$.

*Critical Temperature*

The density of states at the Fermi level is a function of the tilt parameter, which modifies the critical temperature and thermodynamic properties of the superconductor. In particular, in the high temperature regime $T \gg |\Delta|$, the critical temperature can be increased by increasing the tilt parameter (provided $|\beta| \ll 1$). Solving Eq. 3 in these limits, we find that

$$T_c = \frac{2\omega_D \gamma}{\pi} \exp\left[-6(1-6\beta^2/5)/\lambda\nu\right], \tag{5}$$

where $\nu = \mu^2/(2\pi^2 v_z v_\perp^2)$ is the electronic density of states at the Fermi energy per pseudospin and per valley in the absence of tilt and $\omega_D$ is the Debye frequency, which we assume to be independent from the tilt parameter. At large tilt $|\beta| \gg 1$, the critical temperature exponentially vanishes with further increases of the tilt:

$$T_c = \frac{2\omega_D \gamma}{\pi} \exp\left[-|\beta|/\lambda\tilde{\nu}\right], \tag{6}$$

where $\tilde{\nu} = \frac{k_0^2}{8\pi^2 v_z}$ and $k_0$ is the momentum cut-off of the unbounded electron-hole pockets, which itself depends on the tilt parameters, [19]. Such a cut-off is an artifact of the linearized model only, and thus does not arise in our tight-binding calculations given is Section IV. Dependence of the critical temperature $T_c$ and the gap function $|\Delta|$ on the tilt parameter $\beta$ is shown in Fig. 1.

We also note that the important corrections to $T_c$ might come from the many body effects in the case of large tilts. Indeed, the tilt increases the density of states at the Femi level. Thus, the tilt modifies both the electron-phonon interaction parameter and the screening of the electron-electron interaction potential. We consider vertex corrections for the electron-phonon scattering within Migdal approximation $\omega_D/\mu \ll 1$. However, the increase of the density of states increases the screening of the electron interaction potential and thus suppresses the critical temperature in the spirit of McMillan theory. Atomistic and ab initio computations may help to understand more about these complicated issues. We believe that a detailed answer to this fundamental question with accurate treatment of these two interactions goes beyond the scope of our paper.

*Specific Heat*

One of the most fundamental physical quantities in superconductivity is the electronic specific heat, $C$, which at low temperatures can be written as

$$C(T) = 2V \sum_{s=\pm 1} \int \frac{d^3k}{(2\pi)^3} \left[\frac{E_s(\mathbf{k})/2T}{\cosh(E_s(\mathbf{k})/2T)}\right]^2, \tag{7}$$

where $V$ is the volume of sample. In this regime, the specific heat is proportional to the third power of the temperature, $C(T) = \frac{7\pi^2}{15} \frac{\nu V}{|\Delta|^2} T^3(1+6\beta^2)$, reflecting the well known behavior for superconductors with point nodes in the gap [37]. If the Weyl cones are strongly tilted ($|\beta| \gg 1$), and we again consider the low temperature regime ($T \to 0$), this leads to a fully gapped superconducting state, such that the specific heat is now exponentially suppressed and described by the asymptotic behavior: $C(T) \propto \tilde{\nu}|\Delta|^{5/2} \frac{e^{-|\Delta|/T}}{|\beta| T^{3/2}}$.

## III. BULK AND SURFACE STATES

In this section we analyze the quasiparticle spectrum in the bulk of a Weyl superconductor and discuss the presence of any nontrivial surface states. Using the expression in Eq. (4), the eigenvalues of the Hamiltonian in Eq. (2) can be written as $\mathcal{E}_s(\mathbf{k}) = E_s(\mathbf{k} \mp Q\mathbf{e}_z)$. Without loss of generality, we consider the part of the spectrum $E_s(\mathbf{k} - Q\mathbf{e}_z)$, which describes the excitations of quasiparticles in the vicinity of the Fermi sheet enclosing the Weyl point at $\mathbf{k} = (0,0,Q)$. A similar approach can be applied to the Fermi sheet enclosing the Weyl point at $\mathbf{k} = (0,0,-Q)$.

We first examine the limit $\mu = 0$. For $|\beta| < 1$, the spectrum of quasiparticles in the superconductor around the point $\mathbf{k} = (0,0,Q)$ has two point nodes in the gap function at $\mathbf{k} = (0,0,k_{z,\pm})$, where

$$k_{z,\pm} = Q \pm \frac{|\Delta|}{v_z\sqrt{1-\beta^2}}. \tag{8}$$

The increase of the tilt parameter for $|\beta| < 1$ causes $|\Delta|$ to increase as well as the distance between the nodes. The spectrum along the direction of the tilt is given by $E = \pm v_z(1-\beta^2)\delta k_{z,\pm}$, where $\delta k_{z,\pm} = k_z - k_{z,\pm}$. When the Weyl cone is over-tilted, such that $|\beta| \geq 1$, the spectrum of quasiparticles in the superconductor is gapped.

We now consider the case $\mu > 0$. In the range $|\beta| < 1$, the two point nodes in the energy spectrum are located at $\mathbf{k} = (0,0,k_{z,\pm})$, where now

$$k_{z,\pm} = Q + \frac{\mu}{v_z(1-\beta^2)} \left[\pm\sqrt{1+(1-\beta^2)\frac{|\Delta|^2}{\mu^2}} - \beta\right]. \tag{9}$$

The two nodes in the gap function are separated in the momentum space by $|k_{z,+} - k_{z,-}|$. With the increase of the tilt parameter $|\beta|$, this separation grows. For positive (negative) $\beta$, the position of the node at $k_{z,+}$ ($k_{z,-}$) gets closer to the Weyl point $\mathbf{k} = (0,0,Q)$, while the position of the node at $k_{z,-}$ ($k_{z,+}$) diverges to $k_{z,-} \to -\infty$ ($k_{z,+} \to \infty$) as $|\beta| \to 1$. At $|\beta| = 1$, there is only one node at,

$$k_z = Q + \beta\left(1 + \frac{|\Delta|^2}{\mu^2}\right)\frac{\mu}{2v_z}, \tag{10}$$

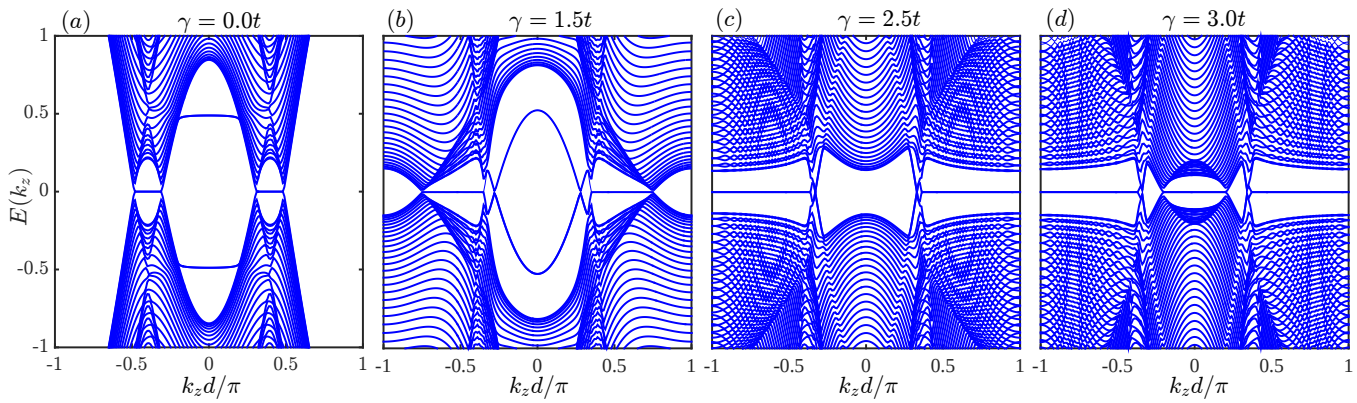


FIG. 2. (Color online) Band structure of the bulk Weyl superconductor as a function of momentum $k_z$ for different values of the tilt parameter $\gamma$ (see Eq. (12)). The energy is normalized by the hopping energy integral $t$. The $x$-axis is directed normal to the two parallel plane boundaries of the superconductor, so that the longitudinal momenta $k_y$ (set to zero here), and $k_z$ are good quantum numbers. The left panel shows the band structure of a Weyl superconductor without tilting, where $\gamma = 0$. The $\gamma$ parameter is increased from left to right as follows: $\gamma = 0, 1.5t, 2.5t$, and $3t$. The chemical potential is fixed at $\mu = 0.5t$ and the superconducting gap is set at $\Delta = 0.2t$. As seen, the region of the Majorana zero energy flat band, bounded to the nodes in the superconducting gap, increases as $\gamma$ increases. When $\gamma = 2.0t$ there is a quantum phase transition, whereby two out of the four gap nodes migrate to the edges of the first Brillouin zone and then reappear at the center when $\gamma \approx 2.7t$. With the further increase of $\gamma$, the Majorana flat band region increases.

at which the spectrum of quasiparticles in the tilt direction in the linear in momentum approximation is given by $\pm v_z \frac{2\mu^2 \delta k_z}{\mu^2+|\Delta|^2}\Theta(\mu^2 - |\Delta|^2)$. Here we note that $\Delta$ is a function of the tilt parameter. The solution for the second node diverges, which means that the linearized model of the Weyl semimetal is no longer applicable in this regime. Instead, one has to take into account the proper band structure of the entire first Brillouin zone so that this spurious divergence can be cut by the momentum corresponding to the edge or center of the first Brillouin zone. We investigate this issue numerically in the next section.

Theoretically, a second node reappears by further increasing the tilt parameter in the region $\sqrt{1+\mu^2/|\Delta(\beta)|^2} > |\beta| > 1$, such that the distance between the nodes $|k_{z,+} - k_{z,-}|$ decreases. Finally, the two nodes merge together when the tilt parameter has the value, $|\beta| = \sqrt{1+\mu^2/|\Delta(\beta)|^2}$, after which a gap opens up in the energy spectrum. We believe that last two conditions could be realized due to proximity effect in the superconductor- Weyl semimetal junctions.

We now briefly discuss the surface states of the Weyl superconductor. There are Majorana zero energy edge modes, which exist along an arc, connecting the nodes of the gap function at $\mathbf{k} = (0, 0, k_{z,-})$ and $\mathbf{k} = (0, 0, k_{z,+})$. For example, at the surface perpendicular to the $x$-direction, the energy spectrum of the Majorana edge modes as a function of the longitudinal momenta $k_y$ and $k_z$, is given by,

$$E_M = \frac{|\Delta| v_z (k_z - Q) v_\perp k_y}{(\mu - \beta v_z (k_z - Q))\sqrt{(\mu - \beta v_z (k_z - Q))^2 - v_\perp^2 k_y^2}}, \quad (11)$$

which is evaluated away from the gap nodes at $\mathbf{k} = (0, 0, k_{z,\pm})$, and satisfies the conditions $v_\perp^2 k_y^2 < (\mu - \beta v_z (k_z - Q))^2$, and $|\Delta| < |\mu - \beta v_z (k_z - Q)|$. In the limit $\beta = 0$, this expression coincides with the one found in Ref. 27. There are two Majorana zero energy flat bands defined by $k_y = 0$ and $k_z = Q$. Tilting of the Weyl cones increases the regions of flat bands in the momentum space along the $z$-axis as $|k_{z,+} - k_{z,-}|$, while the region of flat bands along the $y$-axis in the momentum space diminishes. Having analyzed a few relevant and simple cases, we are now in a position to consider more complicated effects by studying the spectrum of the Majorana flat bands and Fermi arcs numerically.

## IV. NUMERICAL SIMULATIONS

We now investigate numerically the minimal model of a Weyl semimetal with only two Weyl points in the band structure, introduced in Eq. (1). The corresponding tight-binding limit of the Hamiltonian $H(\mathbf{k})$ can be written as

$$H(\mathbf{k}) = (2t\sigma_z - \gamma)(\cos Qd - \cos k_z d) + 2t\sigma_x \sin k_y d - 2t\sigma_y \sin k_x d + m\sigma_z(\cos k_y d + \cos k_x d - 2), \quad (12)$$

where $\sigma$ denotes the spin degree of freedom on each lattice site, $d$ is the lattice constant, and $(t, m, \gamma)$ denote hopping energy integrals between two neighboring sites of the lattice. This choice of Hamiltonian ensures that the zero-momentum inter-valley superconducting pairing is energetically more favorable than the finite momentum intra-valley pairing as discussed in Ref. 28. In

the low-energy limit one can find a correspondence between the lattice and continuum model parameters as $\beta = -\gamma \sin Qd$, $v_z = 2td \sin Qd$, and $v_\perp = 2td$. We note that positive values of $\gamma$, which will be considered further, describe the tilting of Weyl cones in opposite directions. To have a better understanding of the band structure properties and phase transitions in the model Hamiltonian used in Eq. (12), we diagonalize the Hamiltonian along the $k_z$-axis for a bulk material. The resulting eigenvalues are given by:

$$\varepsilon_{\pm,s}(k_z) = \pm 2t(\cos k_z d - \cos Qd) + s\sqrt{(\mu - \gamma(\cos k_z d - \cos Qd))^2 + |\Delta|^2}. \quad (13)$$

The location of the Weyl nodes can be found by determining the roots of Eq. (13), that is, $\varepsilon(k_z) = 0$. The zeros of Eq. (13) are straightforwardly given by

$$k_z^{\pm} = \cos^{-1}\left\{ \frac{(4t^2 - \gamma^2)\cos Qd - \mu\gamma \pm \sqrt{4\mu^2 t^2 + (4t^2 - \gamma^2)|\Delta|^2}}{4t^2 - \gamma^2} \right\}. \quad (14)$$

As seen, the absolute value of the expression in the argument of $\cos^{-1}$ can be larger than unity, depending on the parameters used. Therefore, generally, there arises a region of parameter space in which $\varepsilon(k_z) = 0$ has no solution.

To gain insight into the band structure of the Weyl superconductor, we choose two plane surfaces of the sample to be aligned parallel to each other. The $x$-axis is chosen to be perpendicular to these planes and consequently $k_y$ and $k_z$ are good quantum numbers. This permits exact diagonalization of the model Hamiltonian, Eq. (1). Without loss of generality, we set the superconducting gap to $\Delta = 0.2t$, and choose a nonzero chemical potential of $\mu = 0.5t$. Thus, we do not consider $\Delta$ as a tilting parameter self-consistently. We also define the two Weyl points by setting $Q = 0.4\pi/d$ throughout our numerical calculations.

Figure 2 illustrates the band structure $E(k_z)$ of the system for different tilting strengths $\gamma$ and momentum $k_y = 0$. The behavior of the band structure in the $k_y$ direction is discussed later. As exhibited in Fig. 2(a), when $\gamma = 0$, there are four point nodes in the superconducting gap, with two nodes on each Fermi sheet enclosing two distinct Weyl points. The point nodes are connected pairwise along the $z$-axis in the momentum-space via the flat band at zero energy, corresponding to Majorana surface states. Lines at $E(k_z) \approx \pm\mu$ describe the dispersion of the Fermi arc surface states, which connect two distinct Fermi sheets, consistent with Refs. 27 and 28.

When the tilt parameter $\gamma$ increases within the region $\gamma < 2t$, the outer gap nodes move towards the corners of first Brillouin zone, as seen in Fig. 2(b). At the same time, the Fermi arcs in the particle and hole sectors move towards each other before eventually crossing. This crossing corresponds to the switches of particle-hole symmetric and antisymmetric parts of the Fermi-arcs. From the first term in Eq. (12), it is clear that the flat band reaches the edges of the first Brillouin zone at the phase transition to a type-II Weyl metal at $\gamma \approx 2t$. When $\gamma > 2t$ and the system resides in the type-II Weyl metal phase, we find that the Fermi arcs hybridize with the bulk bands while the two gap nodes connected by a flat band reappear from the center of the first Brillouin zone (Figs. 2(c) and (d)). As seen in Fig. 2(d), for $\gamma = 3.0t$, the Weyl nodes have emerged from the center of first Brillouin zone, and the band structure has a zero mode flat band that connects the Weyl nodes. Focusing on positive values of $k_z$ for concreteness, one observes that the superconducting gap has two nodes in the bulk at $k_z d/\pi \approx 0.23$ and at $k_z d/\pi \approx 0.37$. A zero energy Majorana flat band exists in two intervals: $k_z d \in [0, 0.23]$ and $k_z d/\pi \in [0.37, 1]$ for $k_y = 0$.

In Fig. 3, we present the band structure of a Weyl superconductor again for $\gamma = 3t$, but now as a function of $k_y$ at certain points along the $k_z$-axis. The band dispersion along the $k_y$-axis for $k_z = 0$ is shown in Fig. 3(a). Here, the bulk spectrum is gapped. The two curves that cross zero energy at $k_y = 0$ describe the dispersion of two chiral Majorana states bound to opposite plane surfaces of the Weyl superconductor. At $k_z d/\pi = 0.25$, the bulk states are gapped as shown in Fig. 3(b), while there are two Fermi arcs that cross zero energy at $k_y d/\pi \approx 0.1$. Near the Weyl point $k_z d/\pi \approx 0.37$, Fig. 3(c) shows hints of a flat band in the $k_y$ direction as well. However, as seen, the flat band region is very narrow due to the tilted cones. The rightmost panel, Fig. 3(d), illustrates that the single point band crossing feature is eventually recovered at $k_z d/\pi = 0.5$.

To provide additional details of the bulk and surface state dispersion, in Fig. 4 we present a two-dimensional map of the band structure at energies close to zero. In this figure, the band structure is plotted as a function of $k_y$ and $k_z$ for tilt parameter values ranging from $\gamma = 0$ to $3t$. When $\gamma = 0$, Majorana flat bands exist inside two Fermi sheets enclosing the Weyl points at $\mathbf{k} = (0, 0, \pm Q)$. Namely, in the intervals $k_z d/\pi \in [0.35, 0.5]$ and $k_z d/\pi \in [-0.5, -0.35]$, with $k_y = 0$. There are also flat bands at $k_z d/\pi = Qd/\pi \equiv \pm 0.4$, crossing the $k_z$-axis in the $y$-direction. The two Fermi sheets enclosing the Weyl points are connected by two Fermi-arcs.

With increases of the tilt parameter $\gamma$, Fermi arcs become closer to each other and at $\gamma \approx 0.7t$ touch each other at $k_z = 0$. Increasing $\gamma$ further causes the Majorana flat band at $k_y = 0$ to extend into the $k_z$ direction, while its counterpart at $k_z = 0$ shrinks in the $k_y$ direction. Interestingly, the crossing of the Fermi arcs occurs closer to the gap nodes, which is maximal above the phase transition at $\gamma \approx 2t$. At $\gamma \gtrsim 2.7t$ one observes a reappearance of gap nodes connected by a Majorana flat band in the

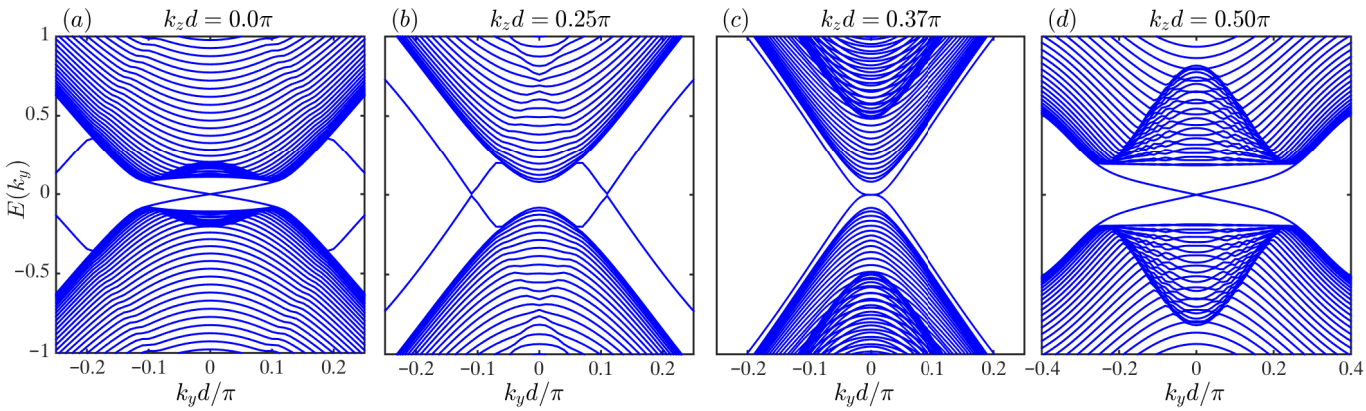


FIG. 3. (Color online) Band structure of the Weyl superconductor as a function of $k_y$ for $\gamma = 3t$ (corresponding to Fig. 2(d)) and for different values of $k_zd/\pi \in [0.0, 0.25, 0.37, 0.5]$. Other parameters are set equal to those of Fig. 2.

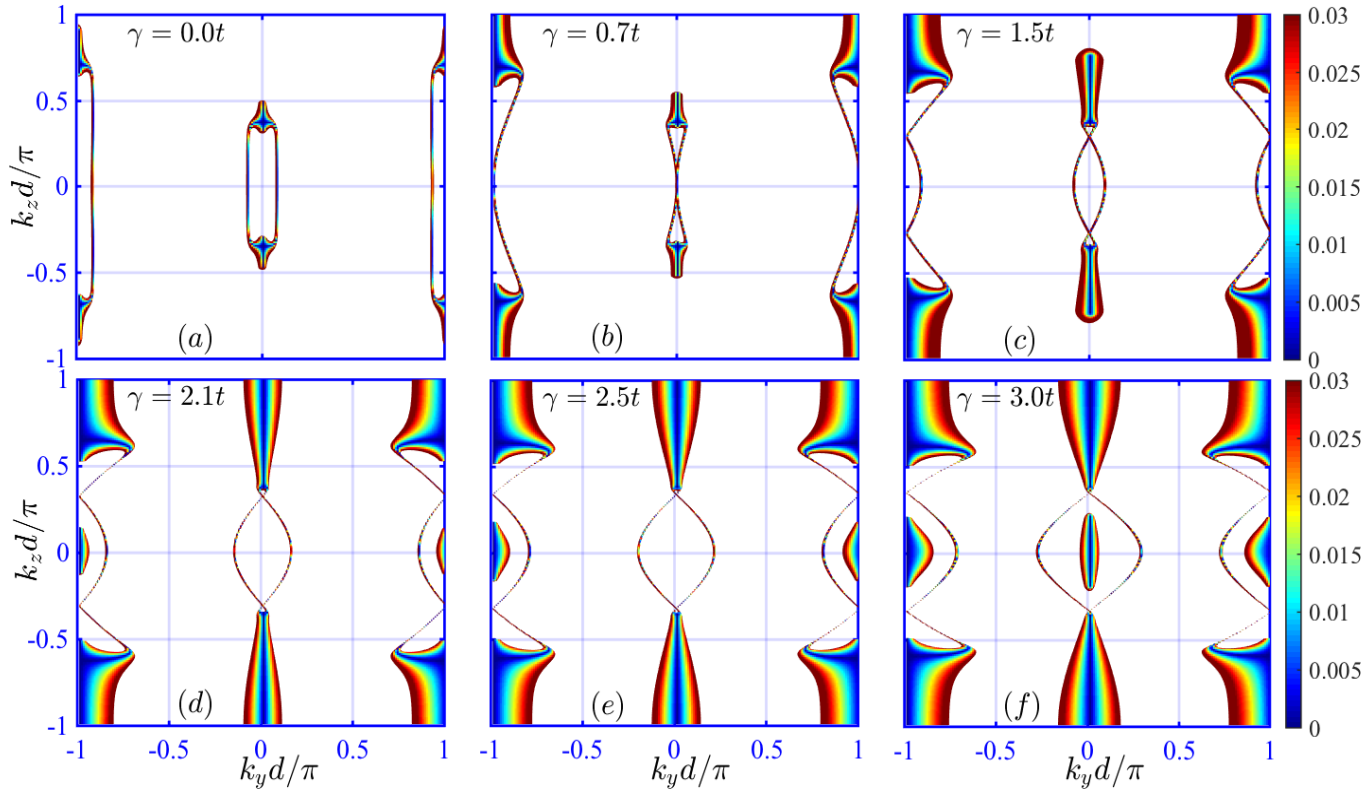


FIG. 4. (Color online) Two-dimensional momentum space map of the band structure at low energies close to zero $E(k_y, k_z) \ll 1$ as a function of $k_y$ and $k_z$. The node titling parameter $\gamma$ evolves from 0 to $3.0t$ corresponding to Figs. 2 and 3. The chemical potential and superconducting gap are fixed at $\mu = 0.5t$ and $\Delta = 0.2t$, respectively.

middle of first Brillouin zone. We note also that a flat band at $k_zd/\pi = \pm Q$ has diminished considerably in the $k_y$ direction.

Thus far we have considered the situation where the tilting parameter is positive, $\gamma > 0$. In the opposite case, $\gamma < 0$, two gap nodes that are positioned closer to the center of the Brillouin zone, move towards $k_z = 0$ as $|\gamma|$ increases. It is evident that the Fermi arcs hybridize directly with the bulk bands without any crossing. The two inner cones finally merge into one and open up a gap, such that only a flat band connecting two outer cones remains. With further increases in $\gamma$, gap nodes reappear from the edges of the first Brillouin zone.

We note that the sign of the chemical potential may play a similar role as $\gamma$, depending on the doping type that is incorporated into the system. Therefore, the zero doping level, i.e. $\mu = 0$, is a specific point. In this regime, the Fermi arcs are degenerate and constitute a

flat band at zero energy connecting the merged cones at zero energy. Increasing $\gamma$ causes splitting of the degenerate Fermi arcs until they hybridize with the bulk bands at values around $\gamma \approx t$. Further increase of $\gamma$ gaps out the touching gap nodes, and finally at large values of the tilting parameter e.g. $\gamma = 3.75t$ we recover two nodes connected by a flat band.

## V. CONCLUSION

We now comment on the effect of tilting the Weyl cones in the same direction, i.e., we consider finite $\alpha$. Note that this tilt breaks inversion symmetry in the system. Thus, it can be easily shown that increasing the tilt parameter $|\alpha|$ suppresses the superconducting gap and decreases the critical temperature, which is opposite to the effect of tilting the Weyl cones in opposite directions to one another.

The effect of tilting the Weyl cones along the same direction is to split each node in the superconducting gap function into two. Taking the limit $\beta \to 0$ together with $|\alpha| > 0$ and $|\alpha| \neq 1$ for concreteness, situates the four point nodes around each Weyl point given by $\mathbf{k} = (0, 0, k_{z,\pm,s})$, where $v_z(k_{z,\pm,s} - Q) = \pm\sqrt{|\Delta|^2 + \mu^2}/(1 + s\alpha)$ and $s = \pm 1$. The spectrum of Bogoliubov quasiparticles along the direction of the tilt is given by $E_{\pm,s} = (\alpha - s)v_z\delta k_z$, bearing a similarity with the type-II Weyl fermions. At the phase transition defined by $|\alpha| = 1$, there are two nodes around each Weyl point. These interesting type-II Bogoliubov quasiparticles could be studied via proximity effect in the superconductor - type-II Weyl semimetal - superconductor junctions.

Finally, the spectrum of Majorana edge states in the limit $|\alpha| < 1$ is given by,

$$E_{M,\pm} = v_z(k_z - Q)\left[\alpha \pm \frac{|\Delta| v_\perp k_y}{\mu\sqrt{\mu^2 - v_\perp^2 k_y^2}}\right]. \qquad (15)$$

Clearly, the flat band at $k_y = 0$ transforms into a linear momentum dispersion.

In conclusion, we have studied superconductivity in a type-II Weyl semimetal. We have found that a quantum phase transition arises whereby the superconducting gap nodes disappear by escaping towards the edges or the center of the first Brillouin zone, and reappearing at the zone's center, or edges, respectively. The regions of Majorana flat bands might be extended as Fermi arcs that connect different Fermi sheets enclosing Weyl points hybridize with the bulk bands. We also note that the superconducting critical temperature and electronic specific heat might be enhanced at the phase transition towards a type-II Weyl state.

## VI. ACKNOWLEDGEMENTS

We thank Anton Burkov for the support of this project. AAZ is financially supported by the Swedish Research Council Grant No. 642-2013-7837 and by the Goran Gustafsson Foundation. K.H. is supported in part by ONR and a grant of HPC resources from the DOD HPCMP

[1] S. Murakami, New Journal of Physics **9**, 356 (2007).
[2] X. Wan, A. M. Turner, A. Vishwanath, and S. Y. Savrasov, Phys. Rev. B **83**, 205101 (2011).
[3] K.-Y. Yang, Y.-M. Lu, and Y. Ran, Phys. Rev. B **84**, 075129 (2011).
[4] A. A. Burkov and L. Balents, Phys. Rev. Lett. **107**, 127205 (2011).
[5] G. Xu, H. Weng, Z. Wang, X. Dai, and Z. Fang, Phys. Rev. Lett. **107**, 186806 (2011).
[6] X. Huang, L. Zhao, Y. Long, P. Wang, D. Chen, Z. Yang, H. Liang, M. Xue, H. Weng, Z. Fang, X. Dai, and G. Chen, Phys. Rev. X **5**, 031023 (2015).
[7] S.-Y. Xu, C. Liu, S. K. Kushwaha, R. Sankar, J. W. Krizan, I. Belopolski, M. Neupane, G. Bian, N. Alidoust, T.-R. Chang, H.-T. Jeng, C.-Y. Huang, W.-F. Tsai, H. Lin, P. P. Shibayev, F.-C. Chou, R. J. Cava, and M. Z. Hasan, Science **347**, 294 (2015).
[8] B. Q. Lv, H. M. Weng, B. B. Fu, X. P. Wang, H. Miao, J. Ma, P. Richard, X. C. Huang, L. X. Zhao, G. F. Chen, Z. Fang, X. Dai, T. Qian, and H. Ding, Phys. Rev. X **5**, 031013 (2015).
[9] C. Zhang, S.-Y. Xu, I. Belopolski, Z. Yuan, Z. Lin, B. Tong, N. Alidoust, C.-C. Lee, S.-M. Huang, H. Lin, M. Neupane, D. S. Sanchez, H. Zheng, G. Bian, J. Wang, C. Zhang, T. Neupert, M. Z. Hasan, and S. Jia, arXiv:1503.02630.
[10] M. Neupane, S.-Y. Xu, R. Sankar, N. Alidoust, G. Bian, C. Liu, I. Belopolski, T.-R. Chang, H.-T. Jeng, H. Lin, A. Bansil, F. Chou, and M. Z. Hasan, Nat Commun **5**, 3786 (2014).
[11] B. Q. Lv, N. Xu, H. M. Weng, J. Z. Ma, P. Richard, X. C. Huang, L. X. Zhao, G. F. Chen, C. E. Matt, F. Bisti, V. N. Strocov, J. Mesot, Z. Fang, X. Dai, T. Qian, M. Shi, and H. Ding, Nat Phys **11**, 724 (2015).
[12] S.-Y. Xu, N. Alidoust, I. Belopolski, Z. Yuan, G. Bian, T.-R. Chang, H. Zheng, V. N. Strocov, D. S. Sanchez, G. Chang, C. Zhang, D. Mou, Y. Wu, L. Huang, C.-C. Lee, S.-M. Huang, B. Wang, A. Bansil, H.-T. Jeng, T. Neupert, A. Kaminski, H. Lin, S. Jia, and M. Zahid Hasan, Nat Phys **11**, 748 (2015).
[13] S.-Y. Xu, I. Belopolski, N. Alidoust, M. Neupane, G. Bian, C. Zhang, R. Sankar, G. Chang, Z. Yuan, C.-C. Lee, S.-M. Huang, H. Zheng, J. Ma, D. S. Sanchez, B. Wang, A. Bansil, F. Chou, P. P. Shibayev, H. Lin, S. Jia, and M. Z. Hasan, Science **349**, 613 (2015).
[14] L. Yang, Z. Liu, Y. Sun, H. Peng, H. Yang, T. Zhang, B. Zhou, Y. Zhang, Y. Guo, M. Rahn, D. Prabhakaran, Z. Hussain, S.-K. Mo, C. Felser, B. Yan, and Y. Chen, Nat Phys **11**, 728 (2015).

[15] Q. Li, D. E. Kharzeev, C. Zhang, Y. Huang, I. Pletikosic, A. V. Fedorov, R. D. Zhong, J. A. Schneeloch, G. D. Gu, and T. Valla, Nat. Phys **12**, 550 (2016).

[16] J. Xiong, S. K. Kushwaha, T. Liang, J. W. Krizan, M. Hirschberger, W. Wang, R. J. Cava, and N. P. Ong, Science **350**, 413 (2015).

[17] G. E. Volovik, *The Universe in a Helium Droplet* (Oxford University Press, Oxford, 2003).

[18] G. E. Volovik and M. A. Zubkov, Nuclear Physics B **881**, 514 (2014).

[19] A. A. Soluyanov, D. Gresch, Z. Wang, Q. Wu, M. Troyer, X. Dai, and B. A. Bernevig, Nature **527**, 495 (2015).

[20] J. Ruan, S.-K. Jian, H. Yao, H. Zhang, S.-C. Zhang, and D. Xing, Nat Commun **7**, 11136 (2016).

[21] D. Gresch, Q. Wu, G. W. Winkler, and A. A. Soluyanov, Arxiv:1611.01858 .

[22] M. Trescher, B. Sbierski, P. W. Brouwer, and E. J. Bergholtz, Phys. Rev. B **91**, 115135 (2015).

[23] A. Zyuzin and R. P. Tiwari, JETP Lett. **103**, 717 (2016).

[24] J. Alicea, Rep. Prog. Phys. **75**, 076501 (2012).

[25] T. Meng and L. Balents, Phys. Rev. B **86**, 054504 (2012).

[26] G. Y. Cho, J. H. Bardarson, Y.-M. Lu, and J. E. Moore, Phys. Rev. B **86**, 214514 (2012).

[27] B. Lu, K. Yada, M. Sato, and Y. Tanaka, Phys. Rev. Lett. **114**, 096804 (2015).

[28] G. Bednik, A. A. Zyuzin, and A. A. Burkov, Phys. Rev. B **92**, 035153 (2015).

[29] L. Yi and F. D. M. Haldane, Arxiv:1510.01730.

[30] Y. Sun, S.-C. Wu, M. N. Ali, C. Felser, and B. Yan, Phys. Rev. B **92**, 161107 (2015).

[31] L. Huang, T. M. McCormick, M. Ochi, Z. Zhao, M. T. Suzuki, R. Arita, Y. Wu, D. Mou, H. Cao, J. Yan, N. Trivedi, and A. Kaminski, Nat Mat **15**, 1155 (2016).

[32] K. Deng, G. Wan, P. Deng, K. Zhang, S. Ding, E. Wang, M. Yan, H. Huang, H. Zhang, Z. Xu, J. Denlinger, A. Fedorov, H. Yang, W. Duan, H. Yao, Y. Wu, S. Fan, H. Zhang, C. X., and S. Zhou, Nat Phys **12**, 1105 (2016).

[33] J. Jiang, Z. K. Liu, Y. Sun, H. F. Yang, R. Rajamathi, Y. P. Qi, L. X. Yang, C. Chen, H. Peng, C. C. Hwang, S. Z. Sun, S. K. Mo, I. Vobornik, J. Fujii, S. S. P. Parkin, C. Felser, B. H. Yan, and Y. L. Chen, arXiv:1604.00139 .

[34] S. Y. Xu, N. Alidoust, G. Chang, H. Lu, B. Singh, I. Belopolski, D. Sanchez, X. Zhang, G. Bian, H. Zheng, M. A. Husanu, Y. Bian, S. M. Huang, C. H. Hsu, T. R. Chang, H. T. Jeng, A. Bansil, V. N. Strocov, H. Lin, S. Jia, and M. Z. Hasan, arXiv:1603.07318 .

[35] K. Koepernik, D. Kasinathan, D. V. Efremov, S. Khim, S. Borisenko, B. Büchner, and J. van den Brink, Phys. Rev. B **93**, 201101 (2016).

[36] Y. Qi, P. G. Naumov, M. N. Ali, C. R. Rajamathi, W. Schnelle, O. Barkalov, M. Hanfland, S. C. Wu, C. Shekhar, Y. Sun, V. Susz, M. Schmidt, U. Schwarz, E. Pippel, P. Werner, R. Hillebrand, T. Forster, E. Kampert, S. Parkin, R. J. Cava, C. Felser, B. Yan, and S. A. Medvedev, Nat. Commun. **7**, 11038 (2016).

[37] V. P. Mineev and K. V. Samokhin, *Introduction to Unconventional Superconductivity* (Gordon and Breach Science Publishers, 1999).